CERN - EUROPEAN ORGANIZATION FOR NUCLEAR RESEARCH

Submitted to
Nuclear Physics B

CERN/EP/PHYS 77-50
26 September 1977

EXPERIMENTAL STUDY OF EXCLUSIVE ONE-PION PRODUCTION IN ALL NEUTRINO INDUCED NEUTRAL CURRENT CHANNELS

Neutrino Propane Gargamelle Collaboration

Aachen-Brussels-CERN-Ecole Polytechnique-Orsay-Padova Collaboration

W. KRENZ, W. LERCHE, J. MORFIN and M. POHL
III. Physikalisches Institut der Technischen Hochschule, Aachen, Germany.

G. BERTRAND-COREMANS, M. DEWIT(*), H. MULKENS(**), C. VANDER VELDE-WILQUET and P. VILAIN(**)
Inter-University Institute for High Energies, U.L.B., V.U.B., Brussels, Belgium.

I. DANILCHENKO(***), D. HAIDT, C. MATTEUZZI and D. PITTUCK(+)
CERN, European Organization for Nuclear Research, Geneva, Switzerland.

P. DEGRANGE, T. FRANCOIS and P. VAN DAM(++)
Laboratoire de Physique Nucléaire des Hautes Energies, Ecole Polytechnique, Palaiseau, France.

D. BLUM, M. JAFFRE, C. LONGUEMARE and C. PASCAUD
Laboratoire de l'Accélérateur Linéaire, Orsay, France.

E. CALIMANI, S. CIAMPOLILLO, G. MIARI and A. SCONZA
Istituto di Fisica dell'Università di Padova, Istituto Nazionale di Fisica Nucleare - Sezione di Padova, Italia.

(*) Boursier IRSIA
(**) Chercheur agréé de l'IISN, Belgique
(***) Now at Serpukhov, and IHEP, USSR
(+) Now at Imperial College, London
(++) Now at NIKHEF, Amsterdam

DH/jr

ABSTRACT

Results are presented on neutrino induced exclusive single pion production in the bubble chamber Gargamelle, filled with a light propane-freon mixture, and exposed to the focused wide-band beam at the CERN PS. The results are corrected for nuclear reinteractions. The isospin structure of the weak neutral current is analysed using all four single pion channels. The isovector-isoscalar interference term is measured and found to differ from zero by two standard deviations. Evidence of Δ production by the weak neutral current is presented. The ratio of π^{o} production by the neutral and the charged current is given.

1. INTRODUCTION

Little is known up to now about the isospin structure and the Lorentz structure of the weak neutral current. The single-pion production in neutrino interactions is one of the simplest reactions to investigate these properties, in particular it can tell, whether the weak neutral current induces isovector or isoscalar transitions. In this experiment all four neutral current induced single pion channels

$$\nu p \rightarrow \nu p \pi^{o}$$
$$\nu p \rightarrow \nu n \pi^{+}$$
$$\nu n \rightarrow \nu n \pi^{o}$$
$$\nu n \rightarrow \nu p \pi^{-}$$

and the charged current induced channel $\nu n \rightarrow \mu^{-} p \pi^{o}$ are measured. The experiment was performed using the bubble chamber Gargamelle filled with a light propane-freon mixture. This liquid is heavy enough to ensure sufficient statistics and good hadron identification; on the other hand, the nuclei, mainly carbon, are light enough to allow a reliable separation of the above channels.

In sect. 2, the event selection, background subtractions and corrections, in particular those due to nuclear effects, are explained. The results are given in sect. 3 together with a discussion of the uncertainties. In sect. 4, a comparison is made of π^{o} production by neutral and charged currents. An analysis of the isospin structure of the weak neutral current is presented in sect. 5. This analysis is based upon all four neutral current channels including, for the first time, the channel $\nu n \rightarrow \nu n \pi^{o}$.

2. EXPERIMENTAL PROCEDURE

2.1 Set-up

The bubble chamber Gargamelle was exposed to the CERN PS wide-band neutrino beam with peak energy around 2 GeV. The beam lay-out was the same as the one described in ref. [1] apart from some additional shielding at the top of the neutrino filter in order to reduce background due to low energy neutrons. The filling of the chamber consisted of propane (C_3H_8) with an admixture of about 10 molar per cent freon (CF_3Br), resulting in a density of 0.54 g/cm^3 and a radiation length of 58 cm. The ratio of free to bound proton targets amounts to 31%. About 85% of the bound nucleons belong to the light nuclei carbon and fluorine. The analysis is based on 276 150 pictures corresponding to 1.21×10^{18} protons on target. This high intensity was achieved with the aid of the PS booster.

2.2 Selection criteria

All films were double scanned for all kinds of interactions. Candidates for six reactions were selected:

- the four neutral current one-pion channels,
- the charged current one-pion channel $\nu n \to \mu^- p \pi^o$,
- the background monitor reaction $np \to pp\pi^-$.

Candidates are defined according to the following criteria:

(a) The interaction occurs inside a fiducial volume of about 3 m^3.

(b) Each candidate has a charge multiplicity compatible with one of the selected channels. Events with an interacting particle of ambiguous charge are rejected.

(c) Events containing a track of projected length less than 2 mm are excluded. Protons above a kinetic energy of about 8 MeV are visible. This requirement eliminates obvious reinteractions in a complex nucleus.

(d) Negative particles with visible capture proton or interacting are called π^-. All other negative particles are called μ^-.

(e) Positive particles are called π^+ if they decay at rest, since the $\bar{\nu}_\mu$ background in the ν_μ beam is at most 0.5%. If they leave the chamber or interact, the ambiguity between π^+ and p can be sometimes resolved by a mass dependent fit on the particle trajectory, by the presence of a δ-ray or, in the case of interacting particles, by characteristic features of the interaction. Stopping protons are unambiguously identified. Positive particles remaining ambiguous are considered proton candidates.

(f) The candidates for the channels $\nu p\pi^o$ and $\mu^- p\pi^o$ must have one or two γ-rays with more than 25 MeV pointing to the vertex with a χ^2 probability of more than 1%. For the channel $\nu n\pi^o$ two γ-rays are required. Whenever two γ-rays are observed, they must have a common origin with a χ^2 probability of more than 1% and an invariant mass between 80 and 180 MeV. The invariant mass distribution of the two γ in $\nu p\gamma\gamma$ events is shown in fig. 1. It has been found in all cases except one that the reconstructed origin of the two γ-rays agrees with the vertex for all candidates $\nu p \to \nu p\pi^o$, $\nu n \to \mu^- p\pi^o$. This demonstrates the reliability of the reconstruction of the π^o vertex also in the absence of charged particles.

The number of selected events for each category is reported in table 1. It is divided into isolated and associated candidates. An event is called associated, if there exists, in the visible volume, a possible upstream source other than a neutral star consisting of identified protons only. The sample of associated events is used to estimate the neutron induced background.

Associated events fitting $\Lambda \to p\pi^-$ have been removed as well as the background of Λ's decaying into $n\pi^o$.

The double scan of the film allows to determine the scanning losses for each category (table 2). In the channel $\nu n \to \nu n\pi^o$ detected only by two γ-rays, it is also important to verify that no systematic loss results from the non-visibility of the neutrino interaction point. A comparison of the $\nu n\pi^o$ and $\nu p\pi^o$ samples is shown in figs 2, 3 and 4.

Neither the spatial distribution nor the energy, nor the angular distribution of the γ-rays indicate any systematic difference. In fig. 5 the momentum distributions of the pions and the protons are presented.

2.3 Background subtractions

The selected sample of candidates is mainly contaminated by two sources of background: hadron interactions and neutrino induced neutral current interactions producing two pions.

A charged hadron entering the chamber and interacting can fake a selected topology. This background is suppressed by removing the events of the appropriate topology for which the momentum along the beam axis is less than 0.6 GeV/c. The signal loss due to this cut was taken into account (table 2). Background due to entering K_L^o is negligible. The only important background due to entering hadrons comes from neutrino induced high energy neutrons. This contamination was determined experimentally in two independent ways.

In a separate run, Gargamelle, filled with the same liquid, was exposed to a monochromatic proton beam of 4 GeV/c [2]. The interacting primary protons give rise to secondary neutrons with a momentum spectrum rather similar to the one in the ν experiment. The selection criteria described above (sect. 2.2) were applied to these neutron interactions. The result of this study is the number of $np\pi^o$, $nn\pi^+$, $nn\pi^o$, $np\pi^-$ and $pp\pi^-$ candidates. The normalization between the two experiments is obtained by comparing the number of candidates fitting the reaction $np \to pp\pi^-$. There are nine $pp\pi^-$ events in the p-experiment and four in the ν-experiment. Although this method is very direct, its statistical uncertainty is large.

The other method is based upon the observed number of associated events (AS) and the ratio B/AS of non-associated (B) to associated (AS) neutron interactions calculated by a Monte-Carlo method. This method has been developed for the neutron background determination in inclusive neutrino induced neutral current interactions and has been verified experimentally [3]. Its application to the conditions of this experiment gives

B/AS = 0.9 ± 0.3; the error includes uncertainties in the energy and angular spectra of the neutrons and uncertainties in the treatment of the nucleon cascade. Before applying the numbers of associated events, as given in table 1, background due to random associations has to be subtracted. From the mean number of events per picture the rate of two independent neutrino like interactions can be determined. It was found, that with a probability of 0.026 a candidate has a random upstream source. This fraction is removed from the sample of associated events and added to the sample of isolated events (table 2). The number of neutron induced background is then B/AS times the corrected number of associated events.

The neutron background determinations by the two methods agree channel by channel within one standard deviation. The combined results are given in table 2.

The other important background sources are neutrino induced neutral current interactions with two pions in the final state. Such interactions can fake one-pion topologies, if a π^+ is misclassified as a proton a π^- as a μ^-, a π^o escapes detection or a pion gets absorbed in the nucleus. All these backgrounds were estimated using a partial sample of events with two identified pions, together with the measured pion detection efficiency. The contribution due to pion absorption in the nucleus was calculated using the same Monte-Carlo program as described in sect. 2.5. The results are shown in table 2. The errors come mainly from the statistics of the 2π sample.

Finally, the contribution of the reaction $\bar{\nu}p \to \mu^+ n$ to the channel $\nu n\pi^+$ was estimated from the calculated $\bar{\nu}$ flux.

2.4 Corrections

The sample after these subtractions represents neutrino induced single pion production and has to be corrected for detection efficiencies.

2.4.1 The π^o detection efficiency

The observed number of events with 1, 2, 3 or 4 γ's can be expressed as a function of the γ detection efficiency and the production rates of 1 and 2 π^o. The contribution of events with 3 π^o is negligible. Resolving this overdetermined system leads to a mean γ detection efficiency of (58 ± 2)%, and allows to evaluate the background due to events with 2 π's as shown in table 2. In the case of the 2γ samples which are obtained with a cut in the $\gamma\gamma$ invariant mass (sect. 2.2 (f)) one has to account for a signal loss due to measurement errors which is found to be (14 ± 6)%.

2.4.2 The π^- detection efficiency

Data from the antineutrino propane experiment in Gargamelle [4] were used to measure the π^- detection efficiency. In that experiment most of the negative particles are π^-. The small contamination of μ^- due to neutrinos in the antineutrino beam can easily be taken into account. The result is shown in fig. 6(a) as a function of momentum. The average value of (49 ± 2)% checks well with a similar measurement in the proton exposure [2] giving (48 ± 7)% and with a measurement using π from fitted Λ or K^o decays giving (53 ± 6)% (preferentially low momenta).

2.4.3 The π^+ detection efficiency

An unbiased sample of π^+ tracks is provided by events kinematically fitting the channel $\nu p \to \mu^- p \pi^+$. The π^+ detection efficiency is deduced by applying the criteria stated in sect. 2.2, and shown in fig. 6(b) as a function of momentum. For momenta below 0.2 GeV/c, the detection efficiency is near to 1, since such pions stop in the chamber and decay. For momenta above 0.6 GeV/c the detection efficiency is still (42 ± 9)% mainly due to δ-ray production.

2.4.4 Correction for particles of ambiguous charge

The sample of fitted $\mu^- p \pi^+$ events indicates that (3.5 ± 1.4)% of the protons with momentum above 0.6 GeV/c have a track of ambiguous curvature due to interaction at a short distance from the main vertex. Slow protons are unambiguously identified. Pions rejected because of ambiguous charge are already taken into account in the π^+ detection efficiency. For negative pions the same rejection rate as for π^+ has been assumed :(2.5 ± 1.4)% below 0.2 GeV/c and (7.0 ± 1.5)% above 0.2 GeV/c.

2.5 Nuclear corrections

Most of the neutrino interactions occur on nuclei targets. The influence of nuclear effects on the $N\pi$ system is schematically shown in fig. 7. The $N\pi$ system can leave the nucleus without interaction and preserve its original topology (a). When an interaction occurs (b), then either the original topology is preserved (c), or another $N\pi$ topology arises from charge exchange (d), or the event is lost because of absorption or production of additional particles (e). Finally, background arises from channels with higher multiplicity by pion absorption (f). It is known from the calculations of the Adler group [5] that nuclear corrections for an aluminium target are substantial. In this experiment the nuclear corrections are expected to be much smaller for two reasons: first, most of the bound nucleons belong to the light carbon nucleus, second, only events without apparent nuclear reinteraction of the $N\pi$ system were selected.

A Monte-Carlo simulation was performed in order to study nuclear interactions. The cascade model of R. Serber et al. [6], is the basis of the program. The nucleus is described as a totally degenerate Fermi gas in a square well potential. Fermi motion and Pauli exclusion principle are taken into account. The model is thus characterized by three parameters only: nuclear radius, potential depth and temperature of the Fermi gas. These parameters have been calibrated by comparison of Monte-Carlo predictions with measurements of hadron nucleus inelastic cross sections.

The most sensitive parameter is the nuclear radius, whereas the other parameters only have a weak influence, since the experimental detection of protons is limited to momenta above $\simeq$ 100 MeV/c. The input quantities are the free-particle cross sections for NN and πN scattering, which are experimentally known to better than 10%. The model successfully passed several tests covering all the stages indicated in fig. 7.

(a) From the partial sample of $\mu^- p\pi^+$ events the number of interactions occurring on free protons $\nu p_H \to \mu^- p\pi^+$ and on bound protons $\nu p_A \to \mu^- p\pi^+$ without nuclear reinteraction of the $p\pi^+$ system can be kinematically separated. Then the two ratios

$$\frac{(\nu p_A \to \mu^- p\, \overset{+}{\pi})(\text{fit})}{(\nu p_H \to \mu^- p\pi^+)(\text{fit})} = \frac{138 \pm 21}{90 \pm 14} = 1.53 \pm 0.33 \text{ Monte Carlo } 1.44 \pm 0.35$$

and

$$\frac{(\nu p_A \to \mu^- p\pi^+)(\text{total})}{(\nu p_H \to \mu^- p\pi^+)(\text{fit})} = \frac{185 \pm 23}{90 \pm 14} = 2.06 \pm 0.41 \text{ Monte Carlo } 2.50 \pm 0.50$$

test the total interaction probability and the probability for conserving the topology (stages a, b, c) respectively.

(b) In a $\bar{p}$ exposure of Gargamelle, filled with a similar liquid mixture, nuclear interactions of pions were studied experimentally in a completely model independent way [7]. The total pion interaction probability inside carbon nuclei was found to be 0.35 ± 0.08, in agreement with the Monte-Carlo prediction 0.47 ± 0.05. Also the relative frequencies of the different reaction channels agree within the experimental accuracy with the predicted values. This is a test of the complete pion cascade.

(c) The 4 GeV/c proton exposure of Gargamelle [2] yielded the relative frequencies of the various neutron induced single pion channels. The Monte-Carlo prediction agrees well with the measured ratios. However, the predictions is affected by the big uncertainties on the measured cross sections for free nucleon target. This tests the stages (c), (d) and (e).

(d) The data of a previous neutrino experiment in Gargamelle filled with freon, CF_3Br, were used to measure the relative frequency of pion and proton interactions leading to 0,1 or more visible protons as a function of the momentum of the incoming particle. Again, the Monte-Carlo predictions agree well with the data (fig. 8). This tests stages (d) and (e).

After these successful tests, the Monte-Carlo program was applied to the conditions of this experiment. The input quantities are the measured proton and pion momentum and angular spectra. Then the transition probabilities S_{ij} from an $N\pi$ state i into an observed $N\pi$ state j are predicted for each type of nucleus in the liquid. These are given in the Appendix.

The sensitivity of the matrix elements to the assumptions of the calculations was tested by varying all parameters within one standard deviation. Then, the absolute magnitude is accurate to about 20% including uncertainties in the input spectra used, whereas the relative magnitude is accurate to better than 10%.

3. RESULTS

Table 3 presents the results of this experiment. In column 2 the number of events before nuclear correction is reported from table 2. Applying the nuclear corrections, as indicated in the last section, and taking into account the ratio of neutrons to protons in the liquid yields events numbers proportional to the cross sections which are given in the last column of table 3 (details are given in the Appendix).

The apparent difference in the correction factors for events off protons and neutrons are due to the surplus of free protons in the liquid. As is evident from the matrices given in the Appendix, factors correcting for the nuclear effects never exceed 1.5.

The errors quoted in table 3 are not completely independent. Some uncertainties in the subtractions and corrections are common to different channels simultaneously leading to correlations. The covariance matrix for the relative cross sections is given in table 4 without including the uncertainties in the nuclear matrix. Since the nuclear matrix is an almost diagonal matrix the 10% uncertainty due to charge exchange plays a negligible role on the final cross sections. A systematic increase by 10% of the absorption affects the results for interactions on protons by about 3% less than for interactions on neutrons. Among the cross section ratios which can be deduced from table 3, $\sigma(\nu p\pi^o)/\sigma(\mu^- p\pi^o)$, $\sigma(\nu p\pi^o)/\sigma(\mu^- p^+)$, $\sigma(\nu p\pi^-)/\sigma(\nu n\pi^+)$ were previously reported [8]. The present experiment improves the accuracy by more than a factor of 4.

4. COMPARISON OF π^o PRODUCTION BY NEUTRAL AND CHARGED CURRENTS

This experiment determines up to a constant factor, the single π^o cross sections on protons and neutrons both for neutral and charged currents. With the values of table 3

$$R_o = \frac{\sigma(\nu p\pi^o) + \sigma(\nu n\pi^o)}{2\,\sigma(\mu^- p\pi^o)} = 0.45 \pm 0.08 ,$$

is obtained. The uncertainty due to nuclear corrections for this particular ratio is less than $\pm$ 0.03. The result on R_o is compared in fig. 9 with the prediction by Adler [9] based on the Weinberg-Salam model. No direct comparison with previous experiments [10] is possible, since they are all carried out on complex nuclei and the event selection includes final states with any number of protons. If a correction factor of 1.5 to 2, as predicted by Adler [9], is applied to the uncorrected ratio R'_o measured in the previous measurements, then no violent disagreement is observed.

5. ISOSPIN ANALYSIS

The isospin structure of the weak neutral current is investigated assuming only that it is a combination of an isovector and an isoscalar. The transition amplitudes for single pion production are then described in terms of two isovector amplitudes A_3, A_1 corresponding to transitions to the I = 3/2 and I = 1/2 states of the Nπ system and an isoscalar amplitude S (table 5).

The four amplitudes satisfy a sum rule

$$A(n\pi^+) - A(p\pi^-) = -\sqrt{2}(A(p\pi^o) - A(n\pi^o)),$$

giving rise to four quadrangular inequalities

$$\sqrt{\sigma(n\pi^+)} \leq \sqrt{\sigma(p\pi^-)} + \sqrt{2\sigma(p\pi^o)} + \sqrt{2\sigma(n\pi^o)}$$

and its permutations. They are all fulfilled experimentally.

Before exploiting the full content of the four equations for the three amplitudes following from table 5, several simple hypotheses may be tested:

(a) $A_3 = A_1 = 0$, $S \neq 0$: pure isoscalar.

Then the following rate relations are expected to hold: $\sigma(p\pi^o) : \sigma(n\pi^o) : \sigma(p\pi^-) : \sigma(n\pi^+) = 1 : 1 : 2 : 2$. A χ^2 test with three degrees of freedom testing the compatibility of the measured data with these ratios gives $\chi^2_3 = 30$ corresponding to a confidence level of less than 10^{-4} and excludes this hypothesis as already indicated in a previous experiment [11].

(b) $A_3 \neq 0$, $A_1 = S = 0$: pure isovector 3/2.

This implies $\sigma(p\pi^o) : \sigma(n\pi^o) : \sigma(p\pi^-) : \sigma(n\pi^+) = 2 : 2 : 1 : 1$ and gives $\chi^2_3 = 10$ corresponding to a confidence level of 0.02.

(c) $A_3 \neq 0$, $A_1 = 0$, $S \neq 0$: absence of isovector 1/2.

The best fit for this hypothesis gives $|S|/|A_3| = 1.2 \pm 0.4$ and $\cos\theta(S, A_3) = -0.21 \pm 0.14$ with $\chi^2_1 = 0.5$ corresponding to a confidence level of 0.45.

Isoscalar-isovector interference term: amongst the 4 Nπ final states there are two pairs of charge symmetric states. The two differences:

$$N(p\pi^o) - N(n\pi^o) = - C \text{ Re } S^*(A_3 + \frac{1}{2} A_1) = 120 \pm 60$$
$$N(p\pi^-) - N(n\pi^+) = - C \text{ Re } S^*(A_3 - A_1) = 57 \pm 66$$

are both proportional to S, where C is a common normalization constant. It follows that C Re $S^* A_3 = - 99 \pm 46$ and C Re $S^* A_1 = - 42 \pm 59$. This indicates the existence of a non-vanishing isoscalar contribution at two standard deviations.

A complete determination of three complex amplitudes A_3, A_1 and S from the four measured (relative) single pion cross sections is not possible. However, limits on the relative magnitudes and phases may be obtained by choosing arbitrarily magnitude and phase of any one of them, e.g. A_3. In that case, four independent quantities specify the configuration of the three representative vectors in the complex plane up to an arbitrary rotation and scale factor. Such quantities are, for instance, the ratios of the four cross sections measured above to the cross section σ_3 for pure isospin 3/2 final states. If σ_3 is chosen as free parameter, the end points of the vectors A_1/A_3 and S/A_3 lie on curves for the given set of measured cross sections $\sigma(p\pi^o)$, $\sigma(n\pi^+)$, $\sigma(p\pi^-)$, $\sigma(n\pi^o)$. These curves are shown in fig. 10 for the central values given in table 3. The non-shaded area shows the allowed regions corresponding to 68% confidence level.

From the shape of the Nπ invariant mass distributions (fig. 11) there is evidence that solutions with both A_1 and S dominating A_3 are excluded. Δ production is particularly prominent in the channel $\nu p \to \nu p\pi^o$, which is least affected by distortions due to reinteractions. It should be noted, however, that the distributions contain background at a level of 30%. The mass resolution is about 25 MeV.

6. CONCLUSIONS

In this experiment the relative cross sections of all four neutral current induced single-pion reactions are given as well as single π^o production by the charged current. An isospin analysis of the weak neutral current is presented in terms of a linear combination of an isovector and an isoscalar amplitude. The possible values of the three amplitudes are illustrated in the complex plane. The weak neutral current is not a pure isoscalar. The data favour the hypothesis of an isovector with $I = 3/2$ dominating $I = 1/2$ plus an admixture of an isoscalar. This conclusion is based upon the observations of Δ resonance production and the isovector-isoscalar interference term. The conclusions of this analysis are in qualitative agreement with the Weinberg-Salam theory.

Acknowledgement

We would like to thank the scanning, measuring and computing staff at each of our laboratories for their work. We express our indebtedness to the operational crews of Gargamelle, the neutrino beam and the PS for their efforts. It is a pleasure to acknowledge the work of Drs M. Baldo-Ceolin, J. Blietschau, F. Bobisut, V. Brisson, H. Deden, W.v. Donninck, M. Hagenauer, F.J. Hasert, D. Lanske, F. Mattioli, K. Myklebost, U. Nguyen Khac, J. Olsen, B. Pattison, P. Petiau, F. Romano, J. Sacton, K. Schultze, H. Wachsmuth, H. Weerts and L. Welch. Finally, we are also grateful to Prof. A. Rousset and Dr. P. Musset for their support and encouragement.

APPENDIX

The Monte-Carlo program described in sect. 2.5 was used to calculate the nuclear matrices S(A) for the three nuclei C, F, Br. Each element $S_{ij}(A)$ gives the transition probability of an Nπ state j produced in the nucleus A into an observed Nπ state i. The numerical results for neutral current interactions are as follows:

$$S(H) = \begin{pmatrix} 1.0 & 0 & 0 & 0 \\ 0 & 1.0 & 0 & 0 \\ 0 & 0 & 0 & 0 \\ 0 & 0 & 0 & 0 \end{pmatrix} \quad S(C) = \begin{pmatrix} 0.644 & 0.022 & 0.094 & 0.030 \\ 0.000 & 0.642 & 0.029 & 0.000 \\ 0.026 & 0.007 & 0.647 & 0.000 \\ 0.013 & 0.001 & 0.017 & 0.666 \end{pmatrix},$$

$$S(F) = \begin{pmatrix} 0.586 & 0.020 & 0.102 & 0.027 \\ 0.000 & 0.605 & 0.029 & 0.000 \\ 0.031 & 0.008 & 0.599 & 0.000 \\ 0.011 & 0.001 & 0.024 & 0.632 \end{pmatrix} \quad S(Br) = \begin{pmatrix} 0.282 & 0.024 & 0.075 & 0.028 \\ 0.001 & 0.289 & 0.015 & 0.001 \\ 0.039 & 0.013 & 0.294 & 0.002 \\ 0.014 & 0.005 & 0.021 & 0.348 \end{pmatrix}$$

where the indices i, j run over the Nπ states in the order $p\pi^0$, $n\pi^+$, $n\pi^0$, $p\pi^-$. Writing the four cross sections $\sigma(\nu p \to \nu p\pi^0)$, $\sigma(\nu p \to \nu n\pi^+)$, $\sigma(\nu n \to \nu n\pi^0)$, $\sigma(\nu n \to \nu p\pi^-)$ as a vector $\vec{\sigma}$, then the cross sections on free nucleon $\vec{\sigma}_{free}$ and the number of observed and produced events are related as follows:

$$\vec{N}_{obs} = \alpha \, \Sigma \, w_i \, S(A_i) \, T(A_i) \, \vec{\sigma}_{free}$$

$$\vec{N}_{prod} = \alpha \, \Sigma \, wi \, T(A_i) \, \vec{\sigma}_{free} \, ,$$

where α is a normalization factor and A_i = H, C, F, Br. The quantities w_i = 0.132, 0.615, 0.105, 0.148, resp. for H, C, F, Br, are the weight fractions of each nucleus for the given liquid mixture. The diagonal matrices

$$T(A_i) = \begin{pmatrix} Z_i/A_i & & & \\ & Z_i/A_i & & \\ & & 1-Z_i/A_i & \\ & & & 1-Z_i/A_i \end{pmatrix}$$

account for the probability to have a proton resp. neutron target available in the nucleus A_i. Putting in numbers, one finds $\vec{N}_{prod}$ = 329, 199, 158, 211. Finally the numbers $\vec{N}$ quoted in the last column of table 3 are proportional to the cross sections $\vec{\sigma}_{free}$; for convenience, the proportionality factor has been chosen such that

$$\vec{N} = \alpha\Sigma \frac{1}{2} w_i \vec{\sigma}_{free} .$$

In the case of the charged current channels only data of the reaction $\nu n \to \mu^- p\pi^o$ are available in this experiment. The following rate ratios were used:

$$\frac{\sigma(\nu n \to \mu^- n\pi^+)}{\sigma(\nu n \to \mu^- p\pi^o)} = 0.4$$

$$\frac{\sigma(\nu p \to \mu^- p\pi^+)}{\sigma(\nu n \to \mu^- p\pi^o)} = 2.0 ,$$

obtained from Argonne measurements [12] modified to account for the harder neutrino energy spectrum. Since the charged current nuclear matrix is almost diagonal, changes in these ratios are ineffective.

REFERENCES

[1] F.J. Hasert et al. (Gargamelle Collaboration), Nucl. Phys. B73 (1974) 1.

[2] R. Arosio, D. Haidt and C. Matteuzzi, CERN/TC-L/Internal Note 77-3

[3] W.F. Fry and D. Haidt, Yellow Report CERN 75-1 (1975).

[4] J. Olsen, private communication from the $\bar{\nu}$ propane Gargamelle Collaboration.

[5] S. Adler, IAS Preprint COO 2220-44 (3/75) revised.

[6] R. Serber et al., Phys. Rev. 72 (1947) 1114.

[7] E. Fett et al., Nucl. Instr. and Methods 144 (1977) 109.

[8] L.G. Hyman, Neutrino Conference 1975;
P. Schreiner, Neutrino Conference 1976.

[9] S.L. Adler, S. Nussinov and E.A. Paschos, Phys. Rev. D9 (1974) 2125.

[10] F.J. Hasert et al. (Gargamelle Collaboration), Phys. Letters 59B (1975) 485;
W. Lee et al., Neutrino Conference Aachen 1976;
H. Faissner et al., Neutrino Conference Aachen 1976.

[11] G.H. Bertrand Coremans et al., Phys. Letters 61B (1976) 207.

[12] S.J. Barish et al., Phys. Rev. Letters 36 (1976) 179.

TABLE CAPTIONS

Table 1 Number of selected candidates.

Table 2 Details of subtractions and corrections.

Table 3 Results.

Table 4 Covariance matrix for the relative cross sections.

Table 5 Transition amplitudes.

Table 1

Channel	$\nu p\pi^o$ $1\gamma + 2\gamma$	$\nu n\pi^+$	$\nu n\pi^o$ 2γ	$\nu p\pi^-$	$\mu^- p\pi^o$ $1\gamma + 2\gamma$	$pp\pi^-$
Isolated	240	104	31	94	301	48
Associated	35	17	4	31	12	17

Table 2

Channel	$\nu p\pi^o$	$\nu n\pi^+$	$\nu n\pi^o$	$\nu p\pi^-$	$\mu^- p\pi^o$
Basic sample	240	104	31	94	301
Scan loss	+7.8	+7.3	+1.9	-	-
Random associations	+6.2	+2.7	+0.8	+2.4	+7.8
Incoming charged hadrons	-0 ± 2	-		-2.3 ± 2.3	-2 ± 2
Incoming neutrons	-25.8 ± 9.7	-13.9 ± 4.9	-2.0 ± 2.3	-22.6 ± 7.5	-3.8 ± 2.3
$\nu N\pi\pi$ p/π^+	-18.8 ± 7.7	-	-	-10.0 ± 2.8	-39.6 ± 13.3
$\nu N\pi\pi$ γ's not detected	-16.8 ± 4.8	-5.5 ± 1.2	-2.9 ± 1.3	-3.4 ± 2.4	-34.8 ± 6.8
$\nu N\pi\pi$ 1π absorbed	-3.5 ± 2.5	-3.2 ± 1.3	-0.1 ± 0.1	-1.6 ± 0.9	-4.2 ± 2.1
$\nu N\pi\pi$ μ^-/π^-	-	-	-	-	-12 ± 10
$\bar{\nu}$ interactions	-	-3 ± 2	-	-	-
Clean $\nu N\pi$ sample	189.1 ± 20.6	88.4 ± 11.6	28.7 ± 5.8	56.5 ± 12.9	212.4 ± 25.3
Final corrected sample	248.0 ± 28.5	140.9 ± 23.0	99.2 ± 21.9	134.0 ± 33.0	272.3 ± 33.8

Table 3

Channel	Number of events before nuclear correction	Cross section in arbitrary units
$\nu p \rightarrow \nu p \pi^{o}$	248 ± 29	297 ± 37
$\nu p \rightarrow \nu n \pi^{+}$	141 ± 23	180 ± 31
$\nu n \rightarrow \nu n \pi^{o}$	99 ± 22	177 ± 43
$\nu n \rightarrow \nu p \pi^{-}$	134 ± 33	237 ± 59
$\nu n \rightarrow \mu^{-} p \pi^{o}$	272 ± 34	526 ± 65

Table 4

	$\nu p\pi^o$	$\nu n\pi^+$	$\nu n\pi^o$	$\nu p\pi^-$	$\mu^- p\pi^o$
$\nu p\pi^o$	1351				
$\nu n\pi^+$	-52	943			
$\nu n\pi^o$	-230	52	1864		
$\nu p\pi^-$	193	37	45	3504	
$\mu^- p\pi^o$	352	-383	17	445	4450

Table 5

Channel	Amplitude
$\nu p \to \nu p\pi^o$	$2A_3 + A_1 - S$
$\nu n \to \nu n\pi^o$	$2A_3 + A_1 + S$
$\nu n \to \nu p\pi^-$	$\sqrt{2}(A_3 - A_1 - S)$
$\nu p \to \nu n\pi^+$	$\sqrt{2}(A_3 - A_1 + S)$

FIGURE CAPTIONS

Fig. 1 Invariant mass distribution of the two γ-rays in the basic sample of $\nu p\gamma\gamma$ events.

Fig. 2 Spatial distributions of the γ-rays from $\nu p\pi^o$ and $\nu n\pi^o$ along (X) and perpendicular (Y, Z) to the neutrino beam axis. The two event samples are normalized to each other.

Fig. 3 Angular distribution of the γ-rays from $\nu p\pi^o$ and $\nu n\pi^o$ with respect to the neutrino beam axis.

Fig. 4 Energy distribution of the γ-rays from $\nu p\pi^o$ and $\nu n\pi^o$.

Fig. 5 Momentum distributions of the pions and protons:

(a) π^+ in $\nu n\pi^+$,
(b) π^- in $\nu p\pi^-$,
(c) π^o in $\nu p\pi^o$,
(d) p in $\nu p\pi^-$
(e) p in $\nu p\pi^o$

Fig. 6 Pion detection efficiencies as a function of momentum

(a) for π^-
(b) for π^+.

Fig. 7 Influence of nuclear effects on the $N\pi$ system.

Fig. 8 Relative frequencies of interactions leading to 0,1 or more visible protons (data points: Gargamelle freon experiment, solid lines: Monte-Carlo predictions for F^{19}):

(a) $\pi^- \rightarrow \pi^-$ or π^o without visible proton,
(b) $\pi^- \rightarrow \pi^-$ or π^o with 1 proton,
(c) $\pi^- \rightarrow \pi^-$ or π^o with more than 1 proton,
(d) p → p + no visible proton,
(e) p → p + 1 proton,
(f) p → p + more than 1 proton.

FIGURE CAPTIONS (Cont'd)

Fig. 9 Comparison of the ratio of single π^o production in neutral and charged currents with the prediction of Adler based on the Salam-Weinberg theory. Note that the theoretical curve was obtained for a neutrino energy of 1 GeV.

Fig. 10 The magnitudes and phases of A_1/A_3 and S/A_3 in the complex plane are shown. The regions forbidden by the data at 68% confidence level are indicated by the shaded areas. The solid curves give the solutions of the equations following from table 5 for the cross sections quoted in table 3. The curves are parametrized by σ_3. Each given value of σ_3 determines unambiguously the real parts of A_1/A_3 and S/A_3, however, their imaginary parts only up to a four-fold ambiguity. This is illustrated in the figure together with the labelling of the four solutions. The marks on the branches for solution 1 correspond to 10 equally divided parameter values between σ_3^{min} and σ_3^{max}. Note that Δ dominance, corresponding to values for σ_3 near σ_3^{max}, would restrict the isoscalar amplitude to a region close to the real axis for solutions 1 and 3, similarly the isovector amplitude A_1 for solutions 2 and 4.

Fig. 11 Invariant mass distributions of the $N\pi$ system in the channels $\nu p\pi^o$, $\nu p\pi^-$ and $\bar{\mu} p\pi^o$.

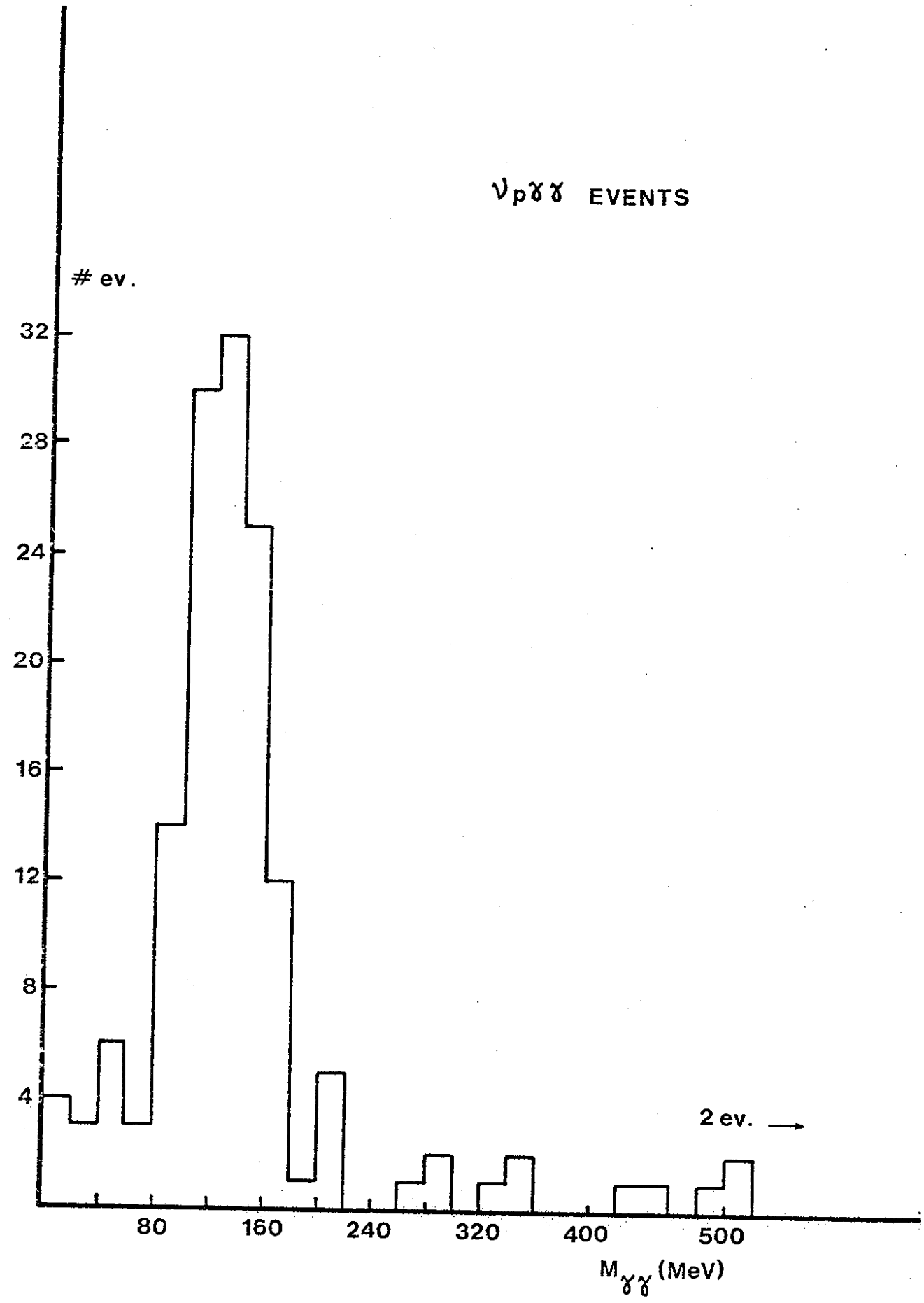
$\nu p\gamma\gamma$ EVENTS
ev.
32
28
24
20
16
12
8
4
2 ev.
80
160
240
320
400
500
$M_{\gamma\gamma}$ (MeV)

Fig. 1

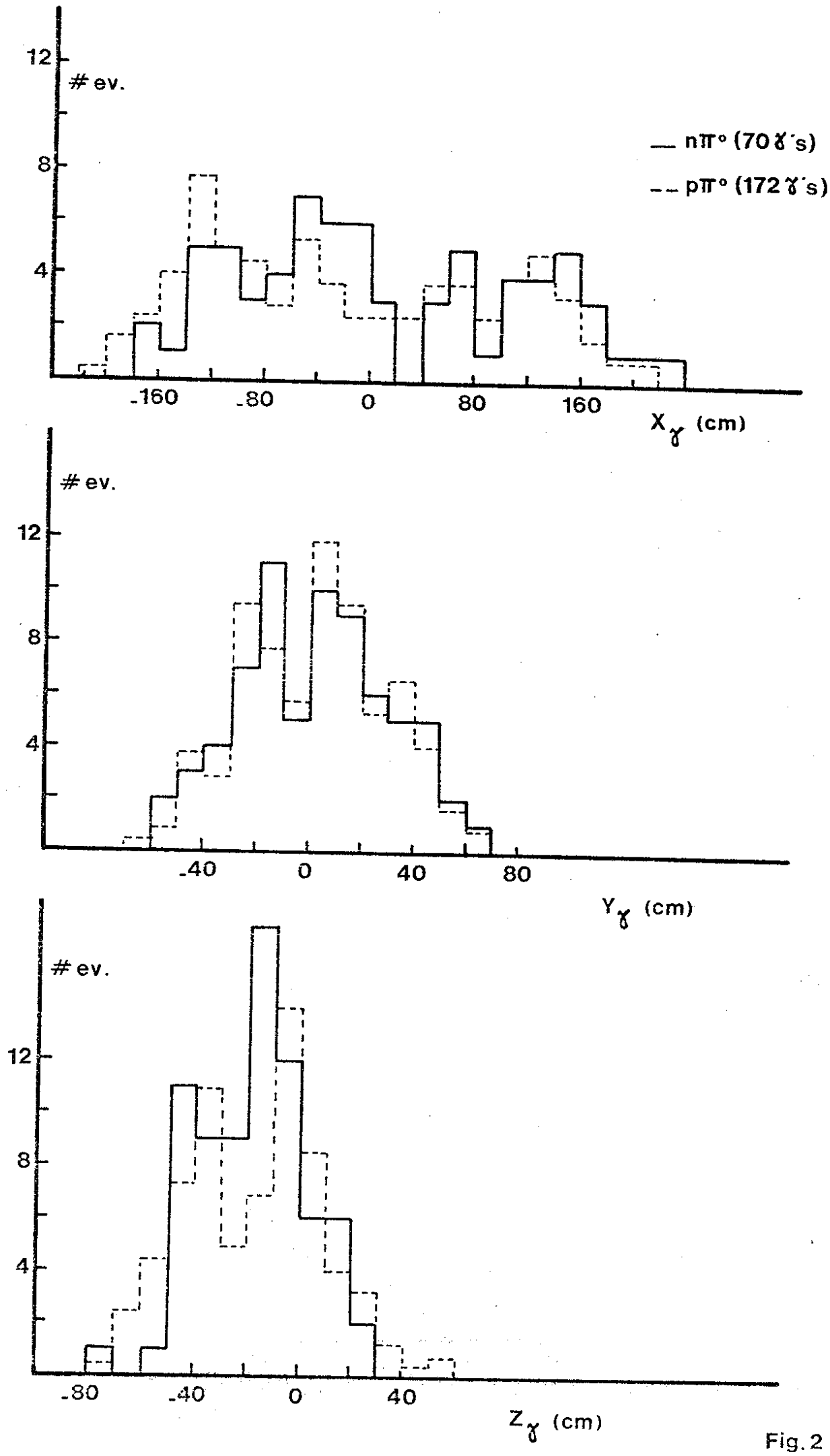
12
ev.
8
4
— nπ° (70 γ's)
-- pπ° (172 γ's)
-160
-80
0
80
160
X_γ (cm)
ev.
12
8
4
-40
0
40
80
Y_γ (cm)
ev.
12
8
4
-80
-40
0
40
Z_γ (cm)

Fig. 2

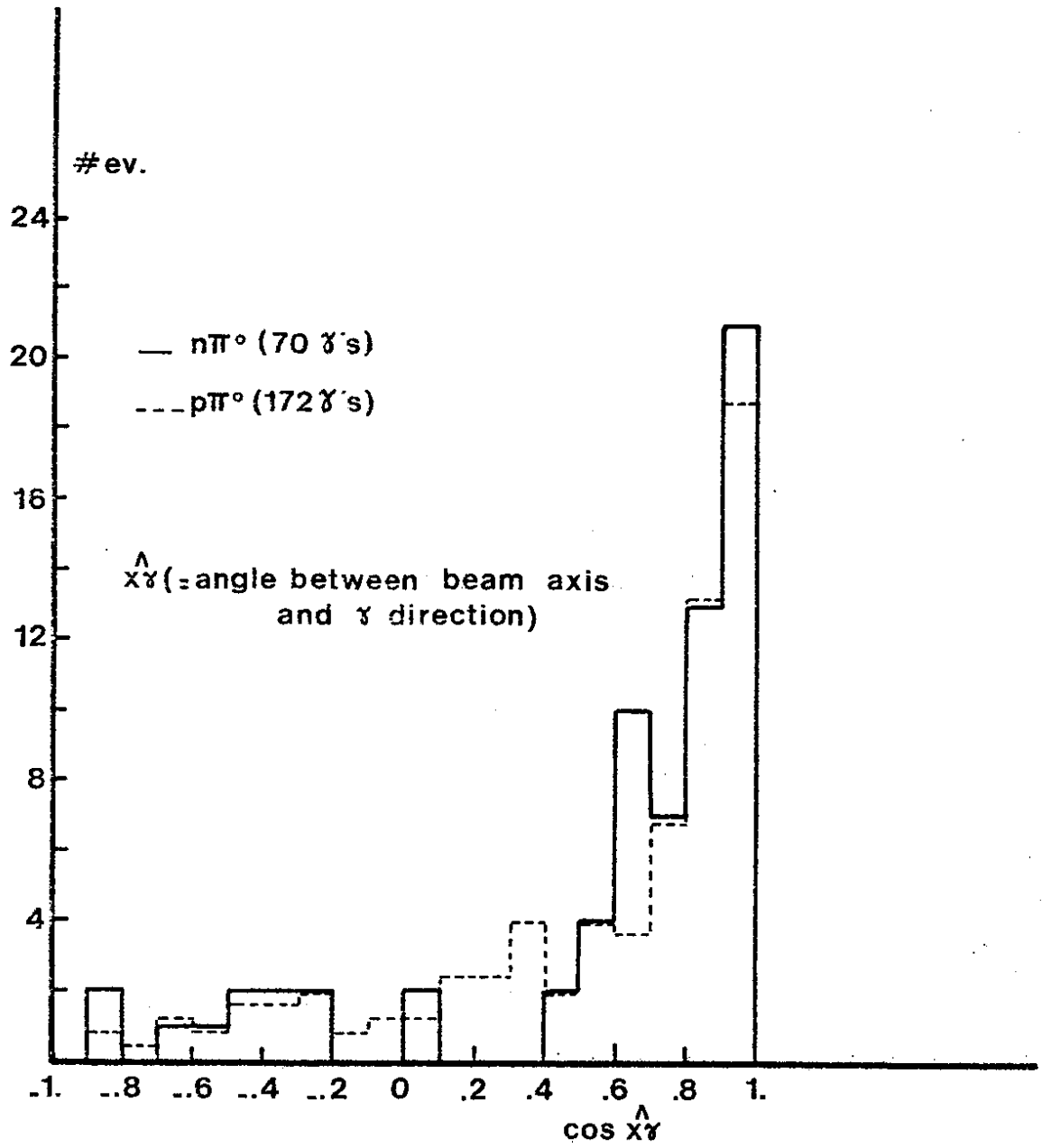
#ev.
24
20
16
12
8
4
— nπ° (70 γ's)
---pπ° (172 γ's)
$\hat{x\gamma}$ (=angle between beam axis and γ direction)
-1.
-.8
-.6
-.4
-.2
0
.2
.4
.6
.8
1.
cos $\hat{x\gamma}$

Fig.3

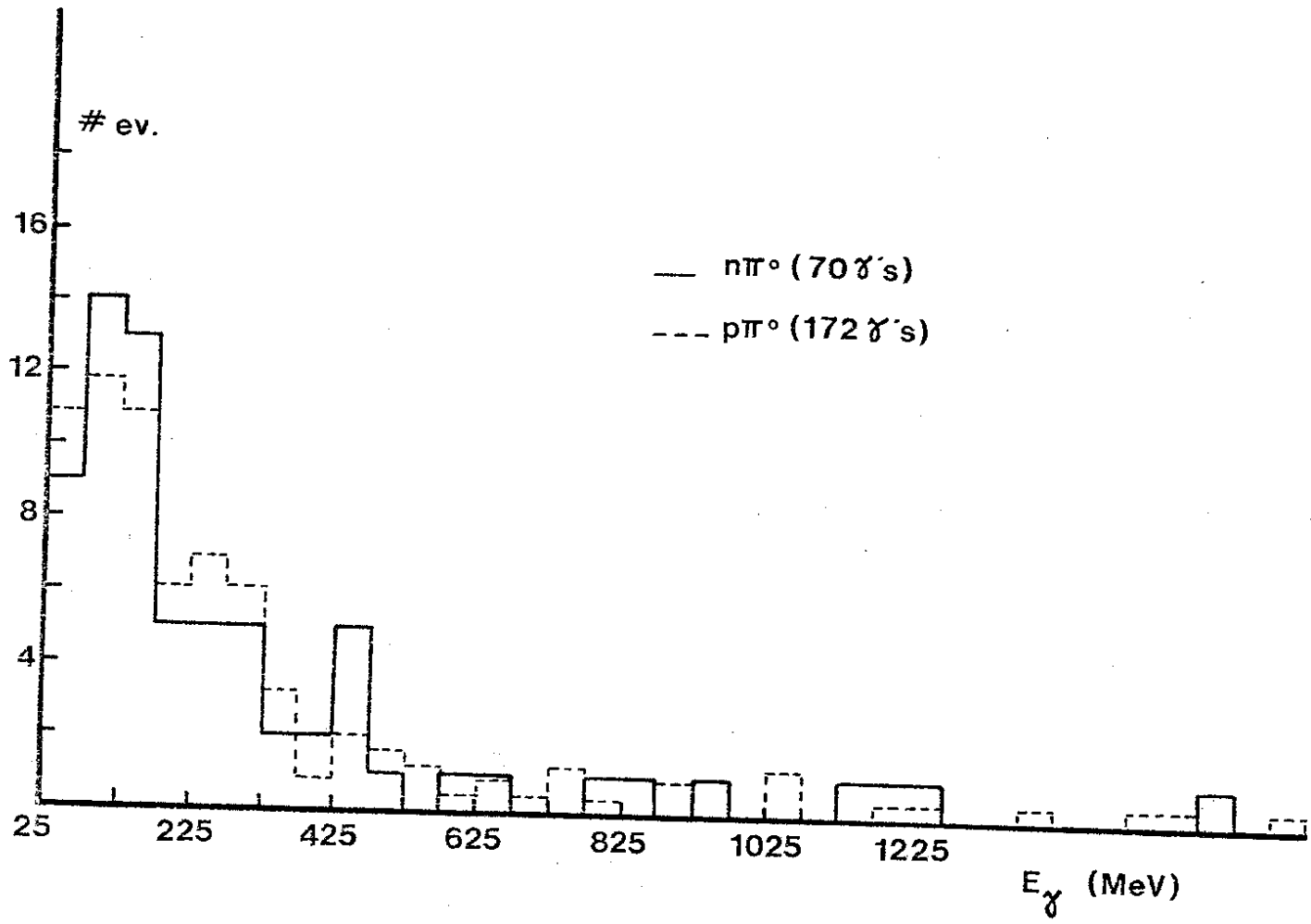
ev.
16
12
8
4
25
225
425
625
825
1025
1225
E_γ (MeV)
— nπ° (70 γ's)
--- pπ° (172 γ's)

Fig. 4

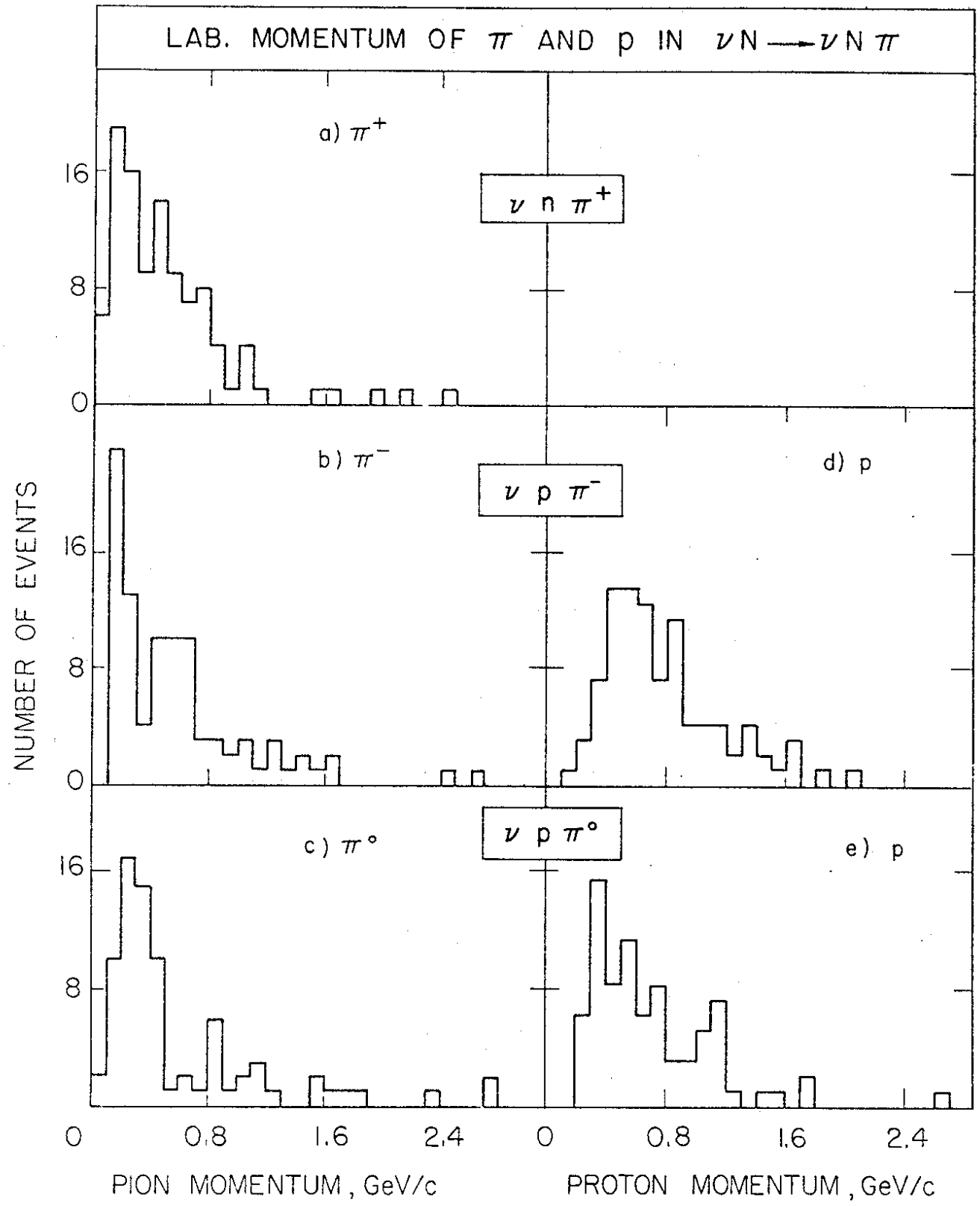
LAB. MOMENTUM OF π AND p IN νN → νNπ
a) π+
ν n π+
b) π−
ν p π−
d) p
c) π°
ν p π°
e) p
NUMBER OF EVENTS
16
8
0
0
0.8
1.6
2.4
PION MOMENTUM, GeV/c
PROTON MOMENTUM, GeV/c

Fig. 5

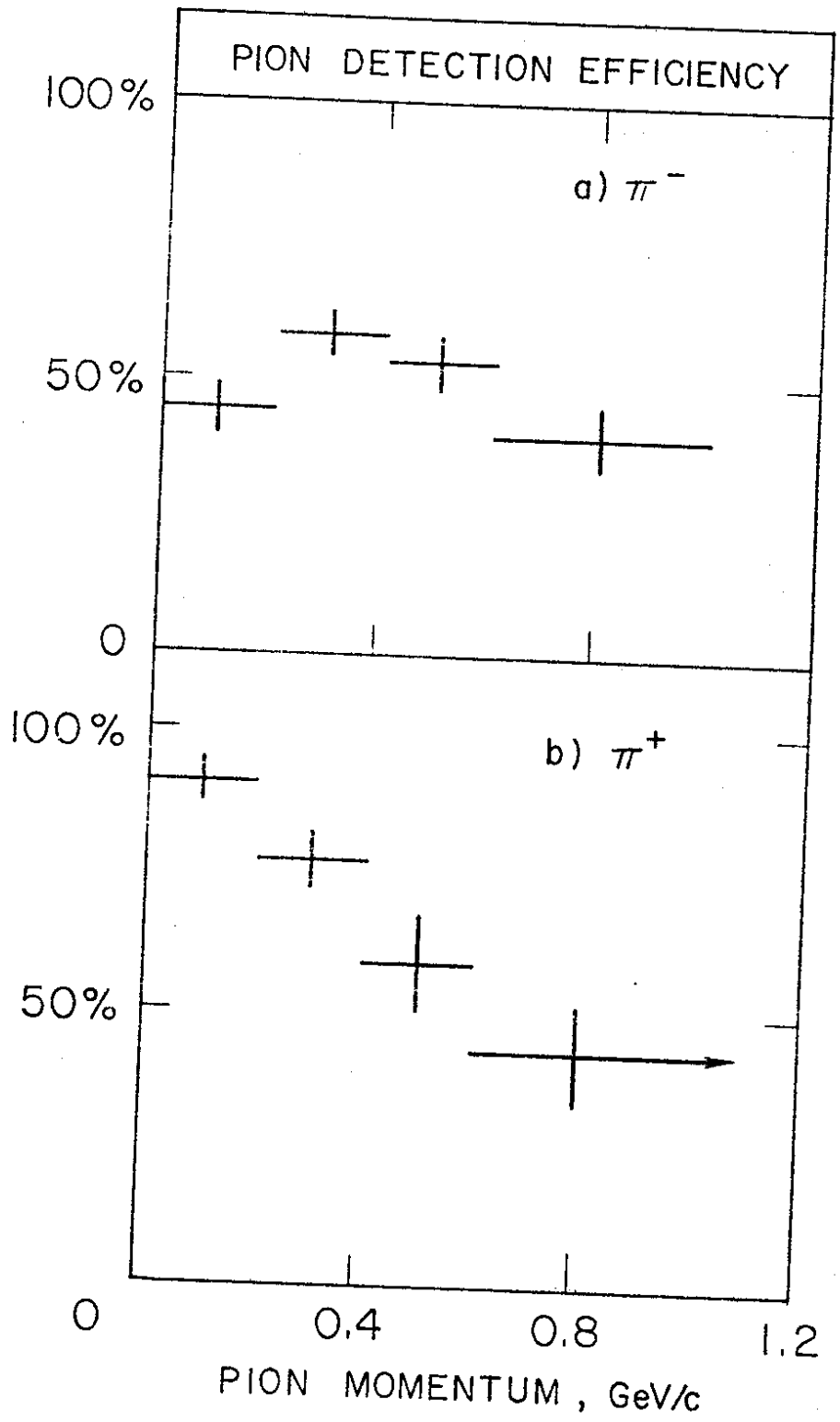
PION DETECTION EFFICIENCY
100%
a) π^-
50%
0
100%
b) π^+
50%
0
0.4
0.8
1.2
PION MOMENTUM , GeV/c

Fig. 6

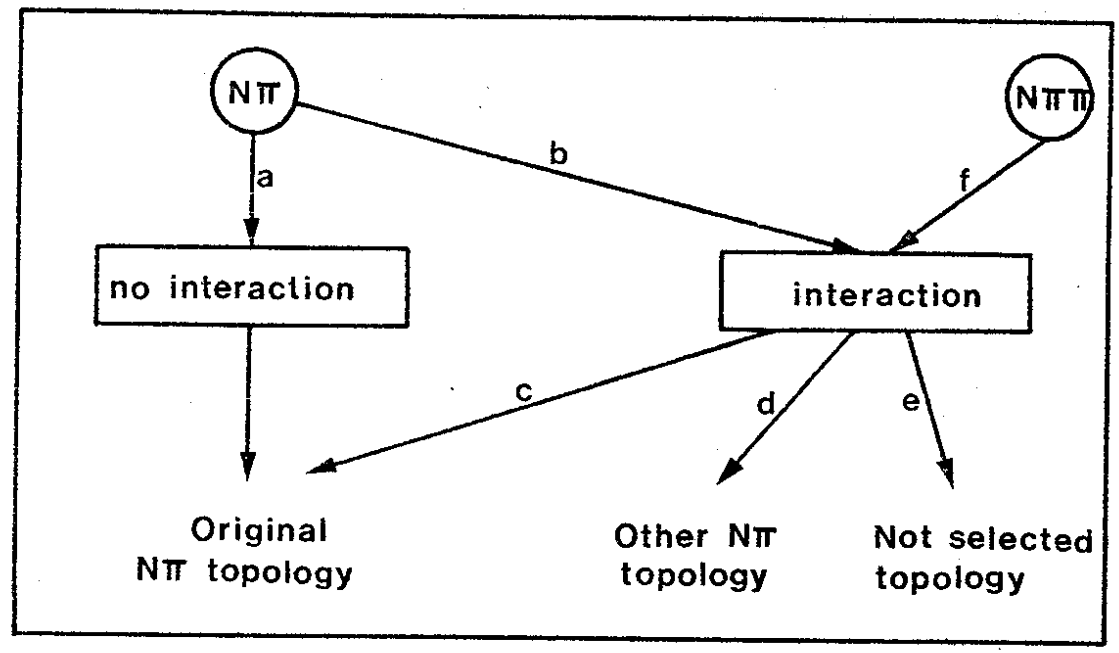
Nπ
Nππ
a
b
f
no interaction
interaction
c
d
e
Original
Nπ topology
Other Nπ
topology
Not selected
topology

Fig.7

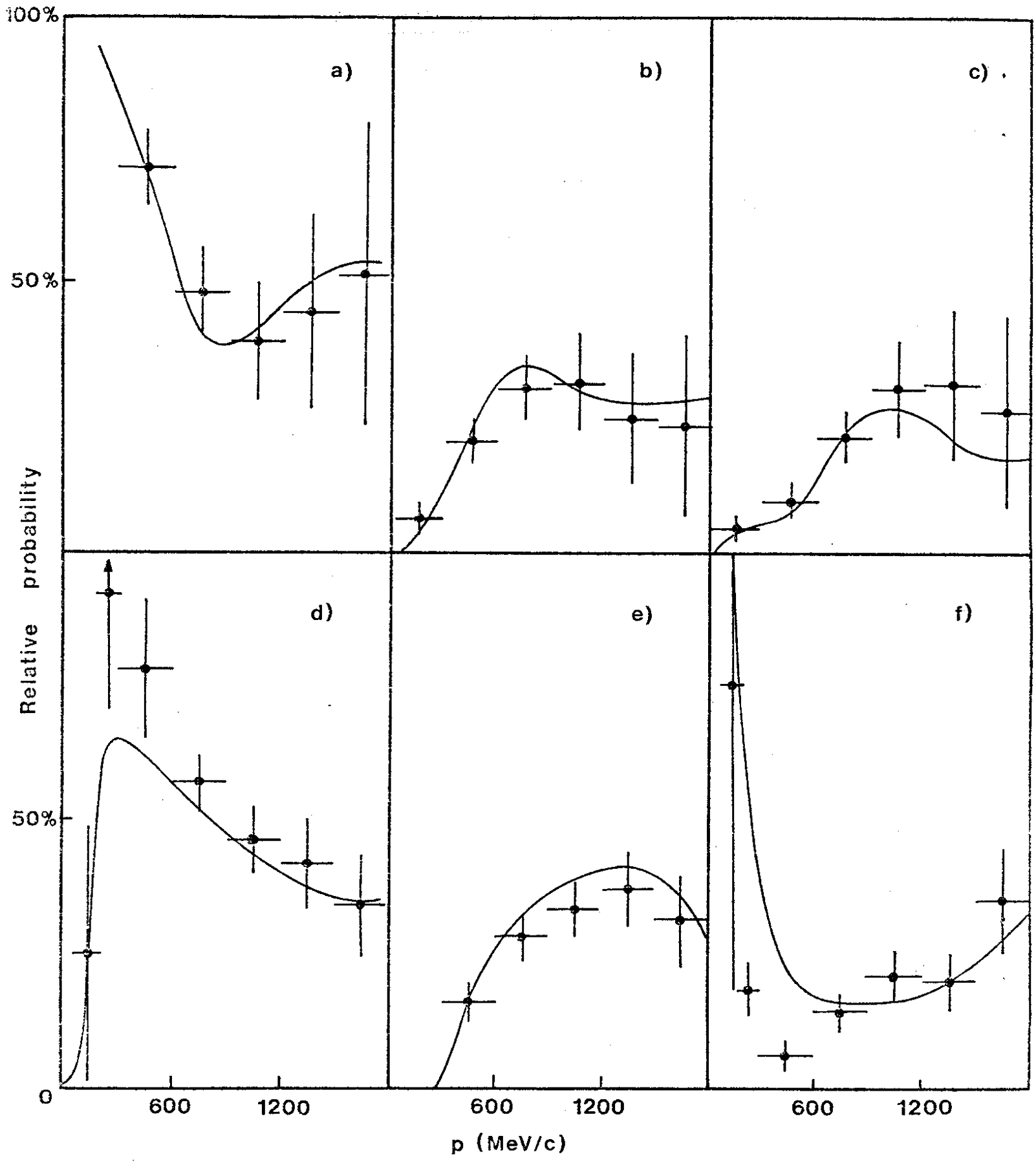
100%
50%
0
Relative probability
a)
b)
c)
d)
e)
f)
600
1200
600
1200
600
1200
p (MeV/c)

Fig.8

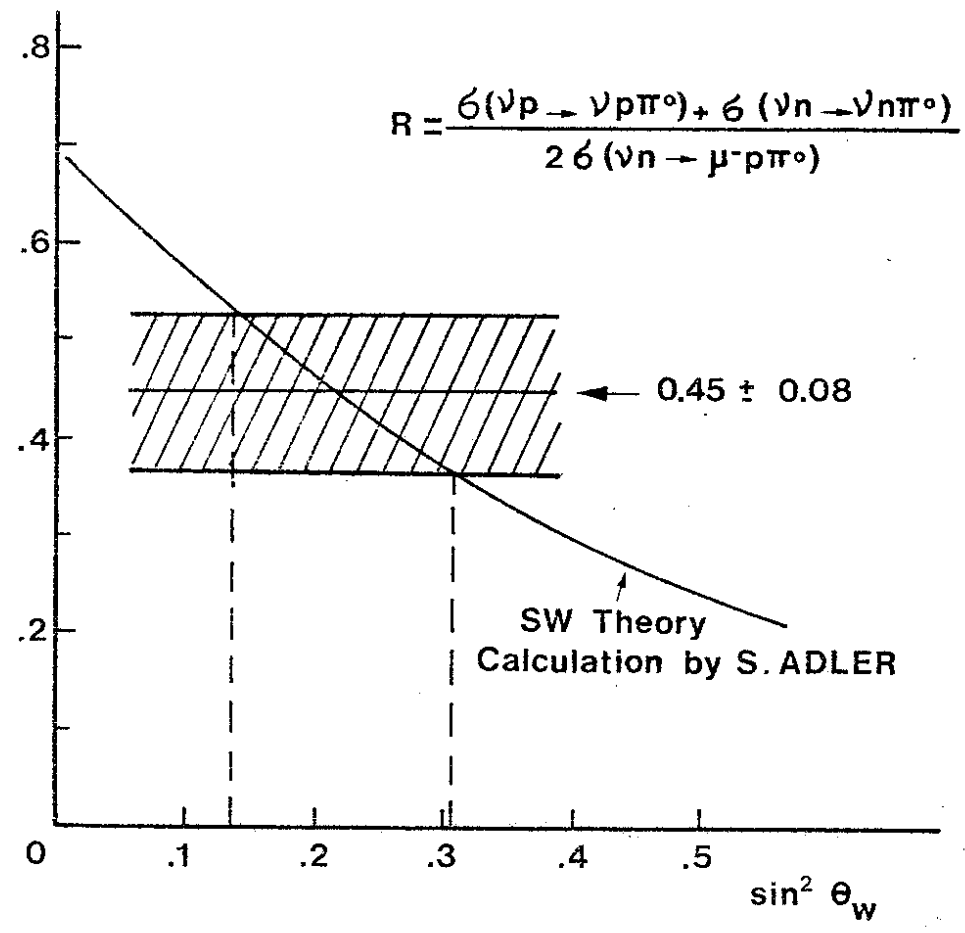
.8
.6
.4
.2
0
.1
.2
.3
.4
.5
$R = \frac{\sigma(\nu p \to \nu p\pi^0) + \sigma(\nu n \to \nu n\pi^0)}{2\sigma(\nu n \to \mu^- p\pi^0)}$
0.45 ± 0.08
SW Theory
Calculation by S. ADLER
$\sin^2 \theta_W$

Fig. 9

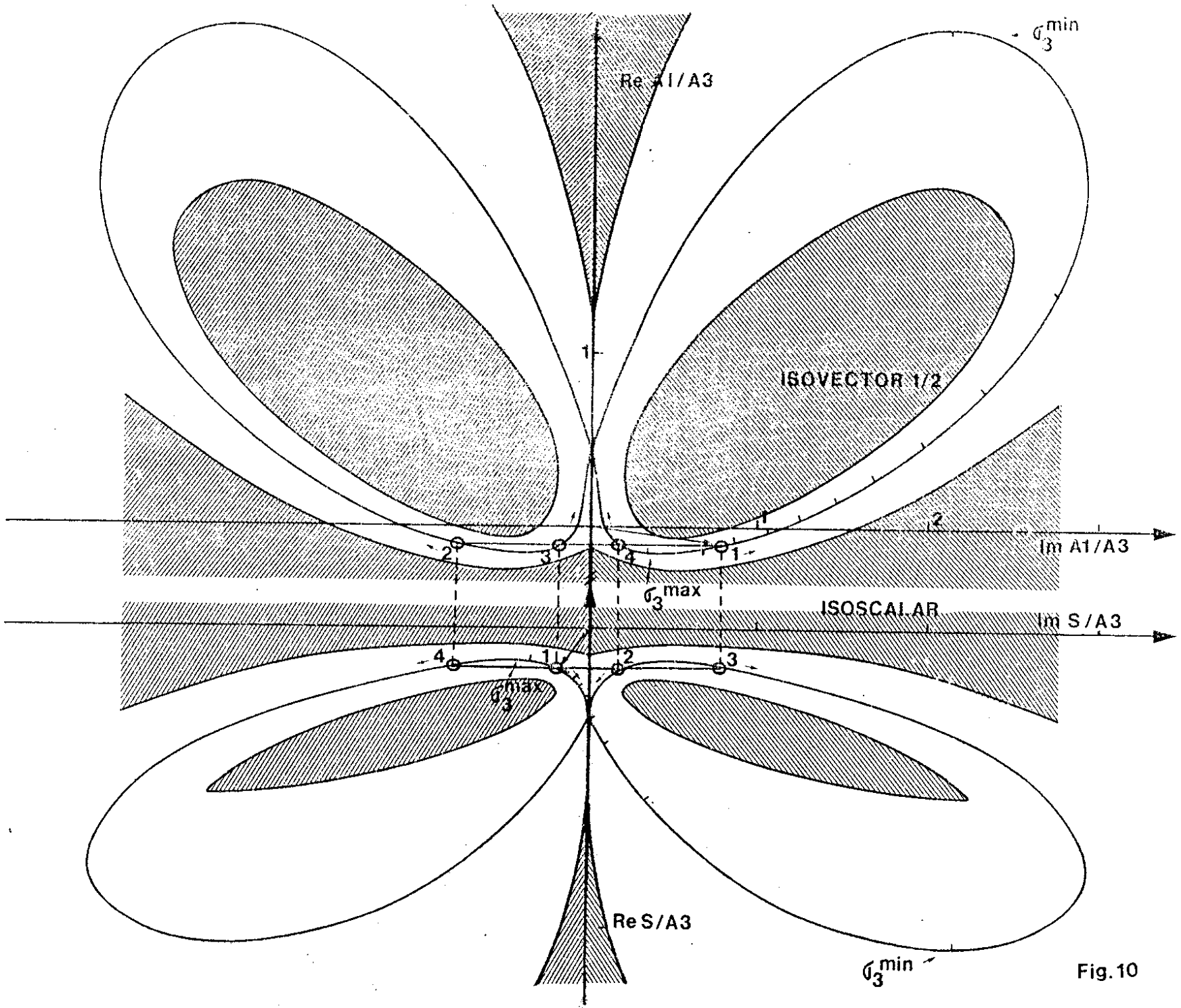
Re A1/A3
σ_3^{min}
1
ISOVECTOR 1/2
1
2
2
3
4
1
Im A1/A3
σ_3^{max}
ISOSCALAR
Im S/A3
4
1
2
3
σ_3^{max}
Re S/A3
σ_3^{min}

Fig. 10

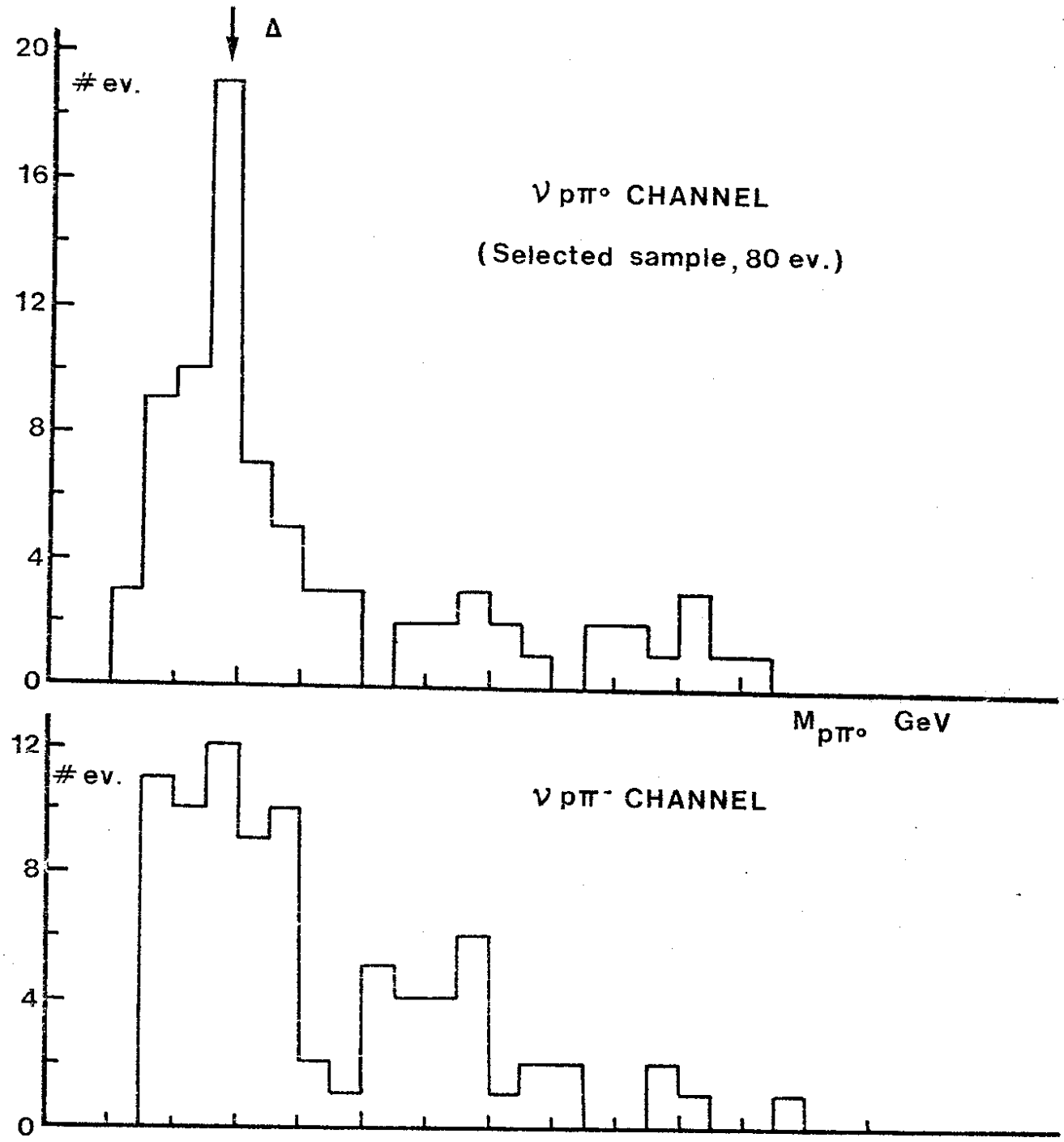
Δ
20
ev.
16
12
8
4
0
ν pπ° CHANNEL
(Selected sample, 80 ev.)
$M_{p\pi^0}$ GeV
12
ev.
8
4
0
ν pπ⁻ CHANNEL
$M_{p\pi^-}$ GeV
16
ev.
12
8
4
0
μ⁻pπ° CHANNEL
(Selected sample, 109 ev.)
1.05
1.25
1.45
1.65
1.85
$M_{p\pi^0}$
2.25
GeV

Fig. 11